

Received April 17, 2019, accepted May 4, 2019, date of publication May 10, 2019, date of current version May 23, 2019.

Digital Object Identifier 10.1109/ACCESS.2019.2916145

A Multi-Stage Model for the Electromagnetic Shielding Effectiveness Prediction of an Infinite Conductor Plane With Periodic Apertures

WANXIN BAI¹, ANQI GUO, TIANLE LI, RUIQI CHENG, AND CHONGQING JIAO¹

State Key Laboratory of Alternate Electrical Power System with Renewable Energy Source, North China Electric Power University, Beijing 102206, China

Corresponding author: Chongqing Jiao (cqjiao@ncepu.edu.cn)

This work was supported in part by the National Key R&D Program of China under Grant 2017YFB0902400, and in part by the Fundamental Research Funds for the Central Universities under Grant 2019MS003.

ABSTRACT This paper focuses on the shielding effectiveness (SE) prediction of the periodic aperture array on an infinite conductor plane against a plane electromagnetic wave with its wavelength much larger than the size of a unit cell of the array. Especially, the existing analytical expressions of SE are combined to cover the entire range of the aperture rate, which is defined as the ratio of the side length of the aperture to that of the unit cell. The combination is carried out by bridging the small aperture model and the wire mesh model. Then, a multi-stage model based on the piecewise function of the aperture rate is presented to calculate the SE for any aperture rate. The model is also extended to consider different wave polarization and incident angles. The results of the model are in good agreement with those from the full-wave simulation. The applicability of the model to a different thickness and aperture shape is discussed. In addition, the upper-limit frequency at which the model is no longer applicable is also analyzed.

INDEX TERMS Aperture array, electromagnetic shielding, shielding effectiveness, wire mesh.

I. INTRODUCTION

Due to widespread applications of electronic devices sensitive to spatial electromagnetic disturbances (EMD), electromagnetic shielding, which is the practice of reducing the electromagnetic field within a space by blocking the field with barriers made of metal materials, as a kind of suppression technique of EMD has been paid extensive attention [1], [2]. The shielding effectiveness (SE) employed to measure the shielding performance is defined as

$$SE = 20 \log_{10}(1/|T|) \quad (1)$$

where, T denotes the insertion loss of a shield and is calculated as the ratio of the electric (magnetic) field intensity with the shield loaded to that with the shield removed.

Electromagnetic shielding effectiveness of an infinite conductor plane with an array of apertures is a classical electromagnetic problem. Numerical methods can be adopted to solve this problem with the advantage of wide feasibility for various aperture shapes, such as square [3], circular [4] and crisscross [5]. However, numerical methods usually have

drawbacks including complex implementation process and large computer memory requirement [6]. Analytical solutions are clear in physical significance and easy to be implemented, while its scope of application is limited to some canonical geometry, such as square [7], circular [8], rectangle [9]. Even so, finding effective analytical solutions or reliable approximate formula solutions remains to be desirable and valuable work.

In the case where the opening area is the same, the shielding effect of the circular and square opening shapes is good because the ratio of the area to circumference is small. In case of circular apertures, the corresponding analytical expression of the SE has been reported [10]. Therefore, we study the electromagnetic shielding problem of an infinite conductor plane with periodic square apertures, as shown in Fig. 1. Wherein, d is the side length of a unit cell, a is the side length of a square, and t is the thickness of the plane. The aperture rate is defined as a/d . When a is significantly smaller than d (a/d tends to 0), the structure can be considered as an array of small apertures. When the aperture is very large (a/d tends to 1), the structure is regarded as a wire mesh, and the SE can be solved by the equivalent circuit model based on the surface impedance of the wire mesh given in [11].

The associate editor coordinating the review of this manuscript and approving it for publication was Kwok L. Chung.

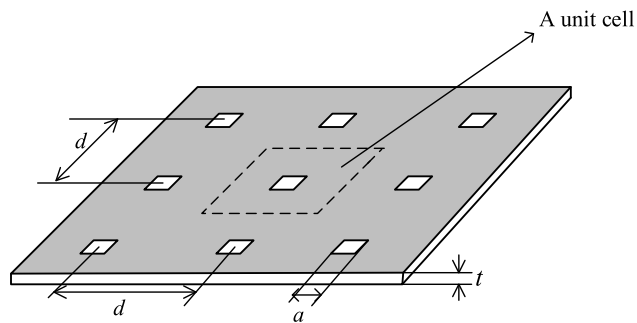


FIGURE 1. Configuration of an infinite conductor plane with periodic apertures.

The calculation of the wire mesh is also mentioned in [12], which is a wire mesh with a circular cross section. Different wave polarization and incidence modes are also analyzed in this paper. However, when the size of the aperture is between the above two extremities, it needs further investigations to find if the above models are still appropriate.

This paper develops a multi-stage model of the SE for the whole interval of $a/d \in (0, 1)$ by bridging the two extremities. The applicability of the model to different frequencies is analyzed. The model is extended to consider different thicknesses, wave polarization, incident angles and opening shapes. This paper is organized as follows. Section II introduces the small aperture model and the wire mesh model and the procedure to develop the multi-stage model of SE is also described in this section. In section III, the application of the model is discussed based on full-wave simulations (CST, Microwave studio [13]). Finally, section IV summarizes the result of this paper.

II. THEORY

A. SHIELDING EFFECTIVENESS OF THE WIRE MESH

When a and d are comparable, the configuration of Fig. 1 can be equivalent to the wire mesh as Fig. 2(a) shown. Fig. 2(b) shows its equivalent circuit. The incident wave is represented by a voltage source with voltage U_0 and internal impedance Z_0 . Wherein Z_0 is the free-space intrinsic impedance. The wire mesh is denoted by two parallel impedances, Z_g and $Z_{g\perp}$. When the direction of electric field component of the incident plane wave is shown in Fig. 2(a), the impedance of the strips parallel to the electric field is represented by Z_g and the impedance of the strips perpendicular to the electric field is represented by $Z_{g\perp}$ [11]:

$$Z_g = j\omega\mu_0(d/2\pi) \ln[1/\sin \frac{\pi(d-a)}{2d}] \quad (2)$$

$$Z_{g\perp} = \pi/[j\omega\epsilon_0 2d \ln(1/\sin \frac{\pi a}{2d})] \quad (3)$$

wherein, ω is the angular frequency. The impedance of the penetration field is described by Z_0 .

We assume that $U_s = 1$. According to Fig. 2, the load voltage is

$$U_L = 1/[Z_0 + 1/(\frac{1}{Z_g} + \frac{1}{Z_{g\perp}} + \frac{1}{Z_0})] \cdot 1/(\frac{1}{Z_g} + \frac{1}{Z_{g\perp}} + \frac{1}{Z_0}) \quad (4)$$

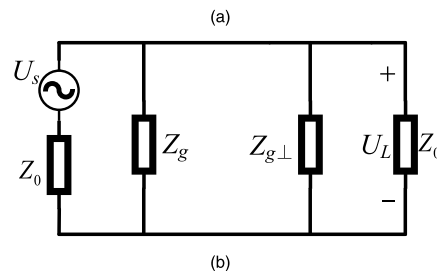
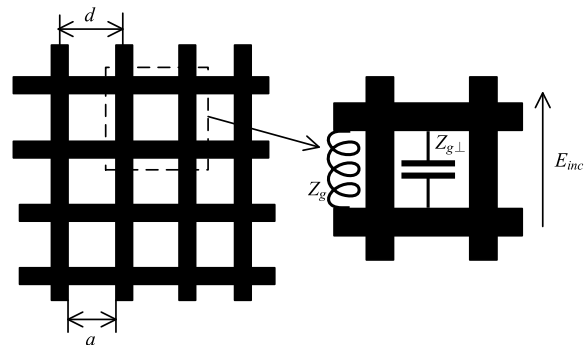


FIGURE 2. Grid of conducting strips with square cells: (a) Configuration. (b) Its equivalent circuit model.

With the conductor plane removed, the corresponding load voltage is $U_0 = 1/2$. Then, T and SE of the wire mesh are defined as, respectively

$$T = U_L/U_0 \quad (5)$$

$$SE_w = 20 \log_{10}(1/|T|) \quad (6)$$

B. SHIELDING EFFECTIVENESS OF THE PERIODIC APERTURES

When a/d is small, Fig. 1 can be considered as the plane with periodic small apertures. Referring to [10], the SE of the plane with arrays of circular apertures for vertical polarization could be expressed as

$$SE_c = 20 \log_{10}(3S\lambda/16\pi r^3) \quad (7)$$

where S is the area of a unit cell, $S = d^2$. λ is the free space wavelength, and r is the radius of a circular aperture.

According to Bethe's theory, the penetration of electromagnetic field through an electrically small aperture could be calculated by using the equivalent dipoles, including an equivalent electric dipole and a magnetic dipole associating with the normal electric field and tangential magnetic field on the aperture surface respectively. Only the equivalent magnetic dipole works for vertical polarization because the normal component of the electric field is zero. The magnetic dipole moment is the product of the tangential magnetic field with the polarization coefficient of the apertures. In [14], the polarization coefficients of circular and square apertures are

$$\alpha_{mc} = 4r^3/3 \quad (8)$$

$$\alpha_{ms} = 0.26a^3 \quad (9)$$

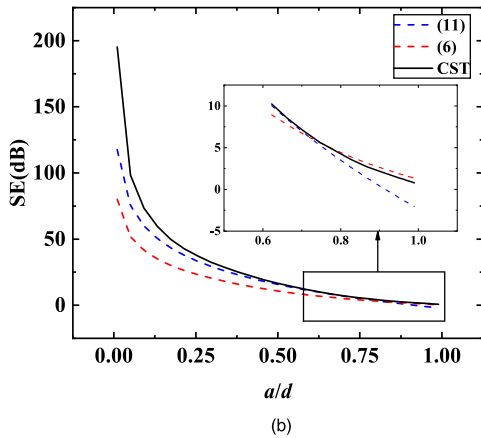
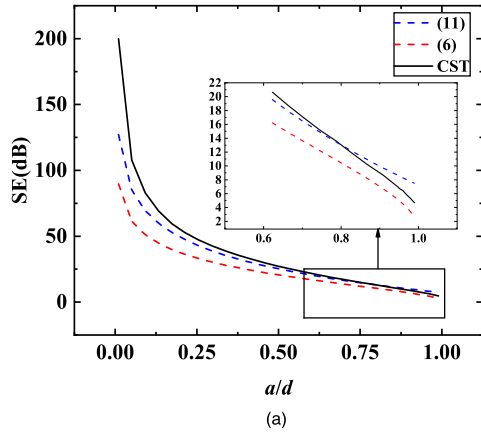


FIGURE 3. Comparison of SE from (11), (6) and full-wave simulation: (a) $f = 1$ GHz. (b) $f = 3$ GHz.

respectively. So (7) can be written as

$$SE_c = 20 \log_{10}(S\lambda/4\pi\alpha_{mc}) \quad (10)$$

By replacing the magnetic polarization coefficient of circular apertures with that of square apertures, the SE for the small square aperture can be calculated by

$$SE_h = 20 \log_{10}(S\lambda/4\pi\alpha_{ms}) = 20 \log_{10}(d^2\lambda/1.04a^3\pi) \quad (11)$$

C. THE PIECEWISE FUNCTION OF SHIELDING EFFECTIVENESS

Fig. 3 shows the SE as a function of a/d with different frequencies. The calculations of SE are carried out by (6), (11) and the full-wave simulation software.

Fig. 3(a) shows that the curve of (6) does not intersect with the curve of (11). The result of the full-wave method is consistent with (11) when a/d is small. After a/d is larger than a value, the simulation result is close to (6). In Fig. 3(b), the two curves have an intersection. Simulation results located on the left and the right of the intersection are close to the calculated results by (11) and (6), respectively. Therefore, the evaluation of the SE is divided into two cases: the two curves based on the above expressions intersect and do not intersect. Next, the premise of existence of intersection is analyzed first.

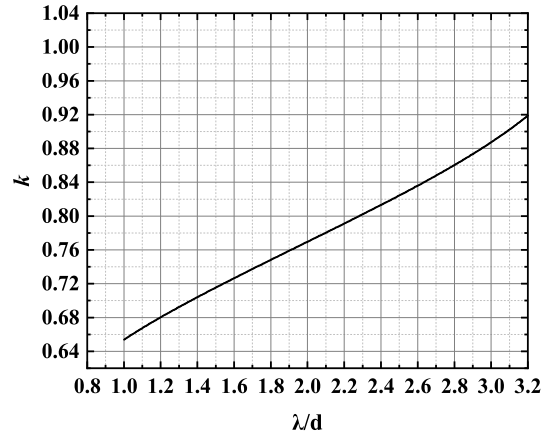


FIGURE 4. The variation of k with λ/d .

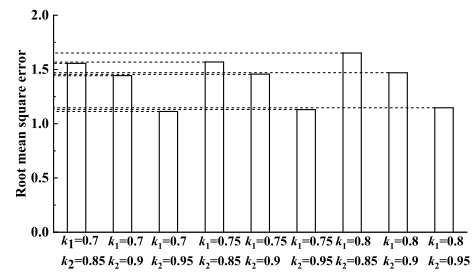


FIGURE 5. Root mean square errors for different combinations of k_1 and k_2 .

It can be deduced that $SE_h > SE_w$ when a/d tends to 0. In case of $a/d = 1$, SE_w is closed to 0 referring to the expressions of surface impedances. If $SE_h < SE_w$, that is $SE_h \leq 0$ at the point of $a = d$, two curves intersect. So $f \geq c/(1.04d\pi)$ is obtained by substituting $a = d$ into $SE_h \leq 0$. Namely, the intersection exists when the frequency is higher than the critical frequency $f_c = c/(1.04d\pi)$.

k is defined as the value of a/d at the intersection where (11) equals to (6). By solving this equality, the variation of k with λ/d is shown in Fig. 4, which reveals that $k > 0.6$ for λ/d from 1 (the premise of (11)) to 3.2 (the premise of existence of intersection). In addition, k is found to be expressed approximately by a linear function of λ/d by

$$k = 0.1156 \cdot \lambda/d + 0.5369 \quad (12)$$

For $f \geq c/(1.04d\pi)$, the SE can be calculated by the two-stage model as following:

- 1) If $0 < a/d < k$, (11) is adopted.
- 2) If $k \leq a/d < 1$, (6) is adopted.

As for $f < c/(1.04d\pi)$, the SE can be calculated by the three-stage model as following:

- 1) If $0 < a/d \leq k_1$, (11) is adopted.
- 2) If $a/d \geq k_2$, (6) is adopted.
- 3) If $k_1 < a/d < k_2$, the linear function is adopted.

$$SE = (SE_w(k_2) - SE_h(k_1)) \cdot (a/d - k_1)/(k_2 - k_1) + SE_h(k_1).$$

Because the results of (11) always agree better with that obtained by the full-wave method only if $a/d < 0.7$,

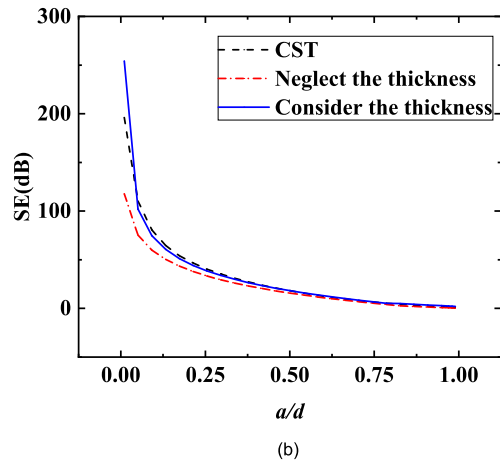
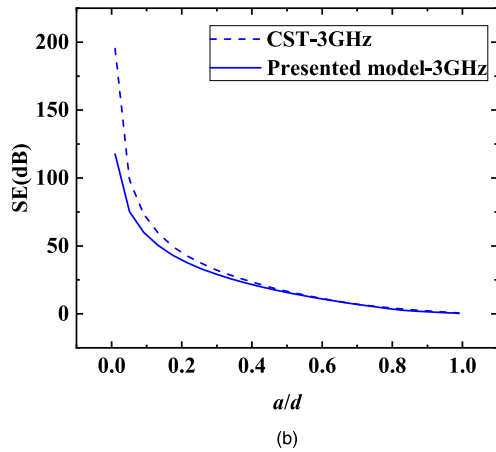
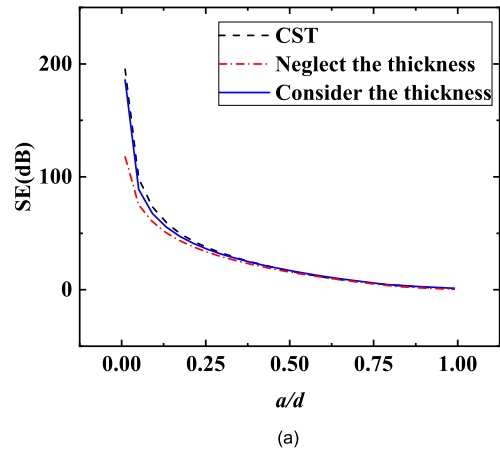
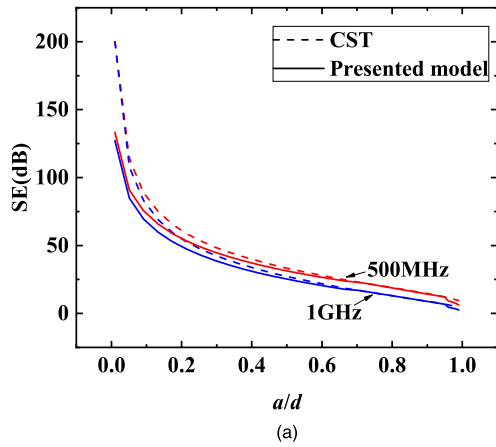


FIGURE 6. Comparison of SE from expressions and full-wave simulation: (a) $f = 500\text{MHz}$ and $f = 1\text{GHz}$, (b) $f = 3\text{GHz}$.

the value of k_1 must not less than 0.7. So k_1, k_2 are selected from 0.7 to 1. The root mean square error (RMSE) is defined as following

$$\text{RMSE} = \sqrt{\sum_{a/d} (\text{SE}_m - \text{SE}_n)^2 / N} \quad (13)$$

In the range of $a/d \geq 0.7$, N different samples are selected with equal interval for calculation. Where SE_m, SE_n are the SE based on the three-stage model and the full-wave simulation, respectively. Fig. 5 shows the dependence of the root mean square error for different combinations of k_1 and k_2 . The optimum values of k_1 and k_2 are 0.7, 0.95, respectively.

III. DISCUSSIONS

A. THE APPLICATION OF THE PIECEWISE FUNCTION

In this part, the case of $d = 4\text{cm}$ is calculated. The critical frequency is 2.3GHz. Fig. 6 shows the SE as a function of a/d with vertical polarization. The three-stage model is employed for 500MHz and 1GHz (Fig. 6(a)), and two-stage model is employed for 3GHz (Fig. 6(b)). When a/d is extremely large (larger than 0.97), the result of the expressions is lightly inconsistent with full-wave simulation results. However, the SE is very poor in this case, which simply means that it is not feasible for practical shielding applications. When

FIGURE 7. Comparison of SE from full-wave simulation, expressions considering the thickness and neglecting thickness for $f = 3\text{GHz}$: (a) $t = 1\text{mm}$, (b) $t = 2\text{mm}$.

a/d is very small (less than 0.01), although the relative error becomes slightly large, the SE has reached more than 200 dB, which is usually much larger than the practical shielding requirement.

B. THE THICKNESS OF THE PLANE

When a/d is small, owing to the influence of depth of the aperture, the cutoff waveguide attenuation should be taken into consideration, from which the SE resulted is given by [15]

$$\text{SE}_{\text{wg}} = \begin{cases} 8.687t \cdot (2\pi/c)\sqrt{(c/2a)^2 - f^2} & f < c/2a \\ 0 & f \geq c/2a \end{cases} \quad (14)$$

where c is speed of light in vacuum, f denotes the frequency of the incident plane wave. SE_{wg} cannot be ignored when f is low, and t is comparable with a . The total SE can be calculated by

$$\text{SE}_{\text{h-new}} = \text{SE}_h + \text{SE}_{\text{wg}} \quad (15)$$

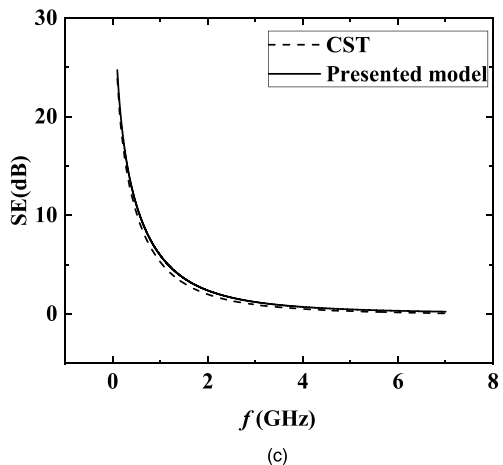
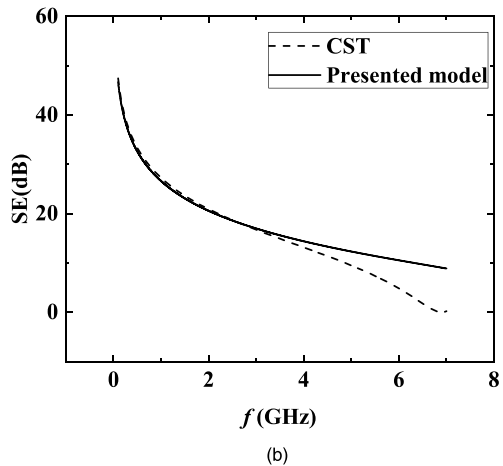
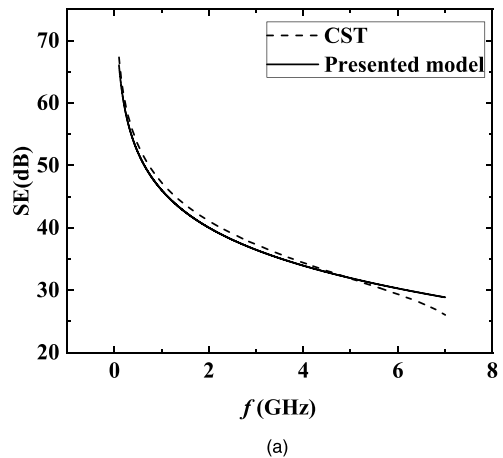
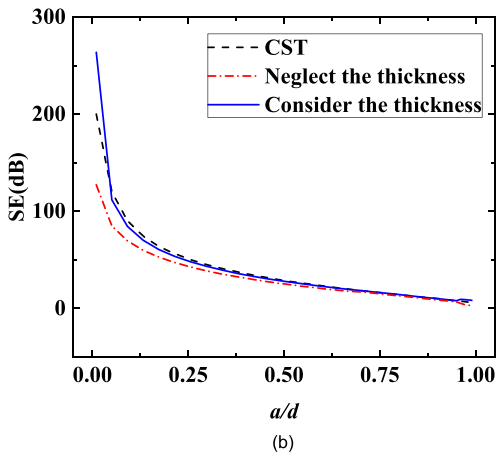
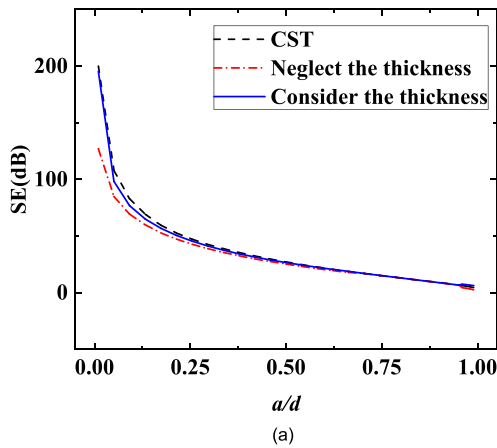


FIGURE 8. Comparison of SE from full-wave simulation, expressions considering the thickness and neglecting thickness of $f = 1\text{GHz}$: (a) $t = 1\text{mm}$, (b) $t = 2\text{mm}$.

As for the wire mesh, taking the influence of thickness into consideration, the effective opening width is calculating as [9]

$$a_{\text{eff}} = a - 5t[1 + \ln(4\pi a/t)]/4\pi \quad (16)$$

When $t = 1\text{mm}$, a_{eff} is about 90% of a , and when t is 2 mm, a_{eff} to a is approximately 80%. The parameter a in (2)-(6) should be substitute by a_{eff} . The SE of wire mesh can be calculated as

$$\text{SE}_{\text{w-new}} = 20 \log_{10}(1/|T_{\text{eff}}|) \quad (17)$$

Fig. 7 compares the result of two-stage model and full-wave simulation for $f = 3\text{GHz}$. For the small aperture model, the accuracy is significantly improved compared to thickness not accounted. As the opening increases, three curves substantially coincide. For the wire mesh model, the difference between the two is not much different from the case of not counting the thickness.

Fig.8 illustrates the SE of $t = 1\text{mm}$ (a) and 2mm (b) versus a/d for $f = 1\text{GHz}$. Similar to two-stage model, the improved effect is obvious when a/d is small. As for a is closed to d , the accuracy of the thickness considered is a little improved compared with the previous one. Therefore, in the following analysis, both the two-stage model and the three-stage model are calculated in consideration of thickness.

FIGURE 9. The SE varies with frequencies: (a) $a/d = 0.25$, (b) $a/d = 0.5$, (c) $a/d = 0.98$.

C. THE FREQUENCY

Fig. 9 describes the variation of the SE with frequency (0.1-7GHz) of $a/d = 0.25, 0.5$ and 0.98 . Equation (15) is adapted for $a/d = 0.25$ and 0.5 , and (17) is adapted for $a/d = 0.98$. In general, the SE decreases with increasing frequency. For $a/d = 0.25$, the difference between results of the full-wave simulation and the expressions is less than 10%. For $a/d = 0.5$, when the frequency is less than 3.75GHz ($\lambda = 2d$), the difference between results of two methods is less

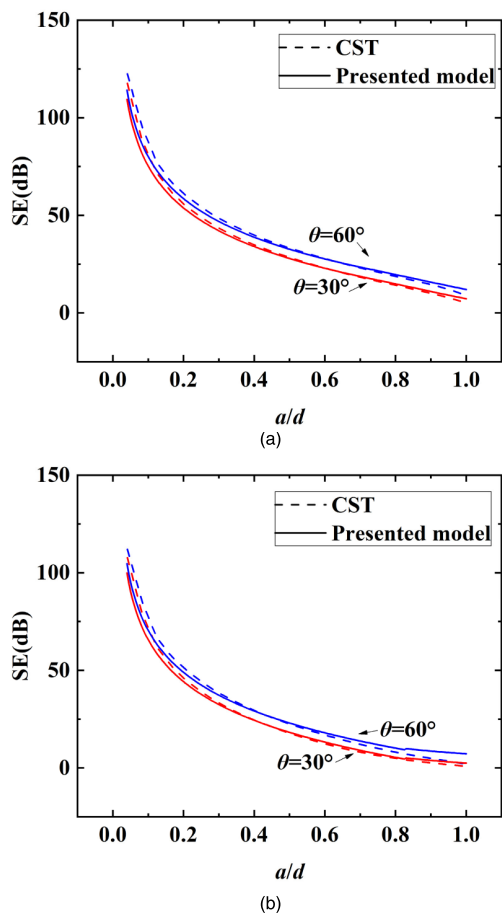


FIGURE 10. Comparison of the SE from expressions and full-wave simulations for perpendicular polarization with different incident angles: (a)1GHz, (b)3GHz.

than 10%. The inconsistency increases with increasing frequency. When $f = 7\text{GHz}$ ($\lambda = d$), the difference is 10 dB, because the premise of the Bethe's theory is $\lambda \gg d$. For $a/d = 0.98$, when the frequency is less than 2GHz, the results of two methods are in good agreement. The SE is almost zero when frequency is larger than 2 GHz, whether the large hole model is effective is of little significance. So, the multi-stage model is applicable for $\lambda \geq 2d$.

D. THE POLARIZATION OF PLANE WAVE AND THE INCIDENT ANGLE

According to [12] and [16], taking the incident angle θ into consideration, the SE of square apertures is given by

$$SE = 20 \log_{10}[1/(|T| \cos \theta)] \tag{18}$$

for perpendicular polarization, and

$$SE = 20 \log_{10} \left\{ \frac{\cos \theta}{|T| [1 - (\sin^2 \theta)/2]} \right\} \tag{19}$$

for parallel polarization.

In Fig. 10 and Fig.11, the incident angel is considered and $t = 1\text{mm}$ is chosen. The SE is calculated as a function of a/d with different incident angels and frequencies for perpendicular polarization in Fig. 10, and for parallel polarization

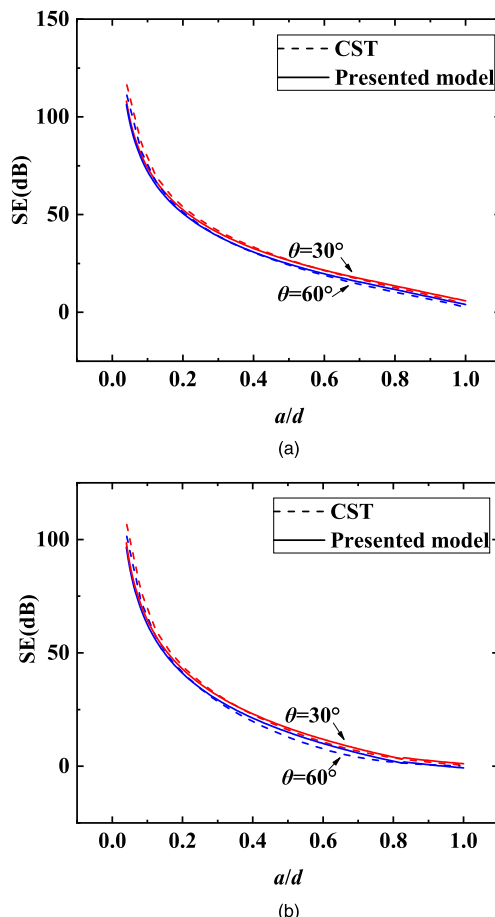


FIGURE 11. Comparison of the SE from expressions and full-wave simulations for parallel polarization with different incident angles: (a)1GHz, (b)3GHz.

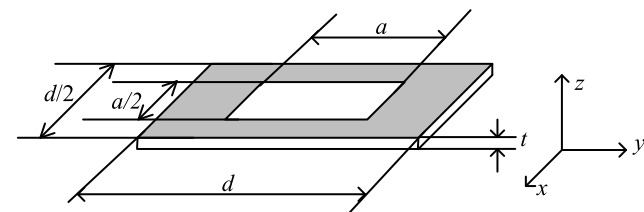


FIGURE 12. Configuration -of rectangle opening with an aspect ratio of 2.

in Fig. 11. The SE does not change much in case of $\theta = 30^\circ$ and 60° . For perpendicular polarization, the SE of $\theta = 60^\circ$ is greater than $\theta = 30^\circ$, and the opposite is shown for parallel polarization. The discrepancy between expressions and full-wave simulations increases as the incident angle increases for perpendicular polarization.

E. THE SHAPE OF THE APERTURE

The case of rectangle opening is presented to analyze the applicability of opening shape for the multi-stage model. For the small aperture model, the polarization coefficient in (10) is replaced with that of the corresponding shape [14]. For the wire mesh model, the parameter a in (2) is substituted by the distance of wires parallel to the electric field and the parameter a in (3) is substituted by that the distance of wires perpendicular to the electric field.

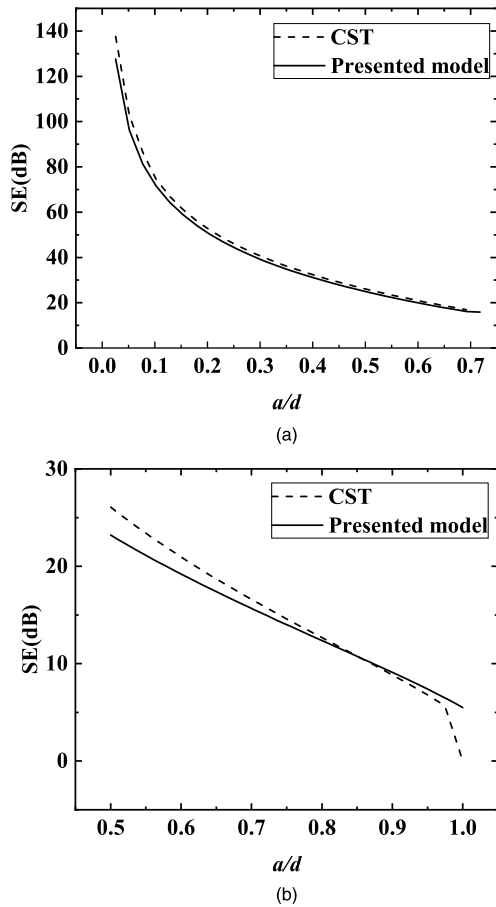


FIGURE 13. Comparison of the SE from full-wave simulation and expressions of $f = 1\text{GHz}$: (a) $a/d = 0 - 0.7$, (b) $a/d = 0.5 - 1$.

Take the example of a rectangle with an aspect ratio of 2 as shown in the Fig. 12. Equation (15) is adapted when a/d is 0 to 0.7. The polarization coefficient of rectangular is substituted into (15) and the results is shown in Fig.13(a) [14]. The difference of results of full-wave simulation and expressions is less than 10% when a/d from 0 to 0.7. Equation (17) is adapted when $a/d = 0.5 - 1$. Assuming that the incident electric field is in the x direction, the parameter a in (2) is the distance of adjacent wires in the x direction, and a in (3) is the distance of adjacent wires in the y direction. Fig. 13(b) shows the results of the full-wave method and expressions. The difference between two methods is less than 3dB except a is extremely closed to d .

The results obtained from the two-stage model and the three-stage model in section II are shown in Fig. 14 for different frequencies. The agreement of two methods for $f = 1\text{GHz}$ is well, so, the three-stage model of $k_1 = 0.7$, $k_2 = 0.95$ is effective in this case. For $f = 3\text{GHz}$, there are some disagreements when a/d is around 0.8 because the calculation of the intersection should be further correction. Therefore, the bridging method in Section II may not be applicable for different opening shapes.

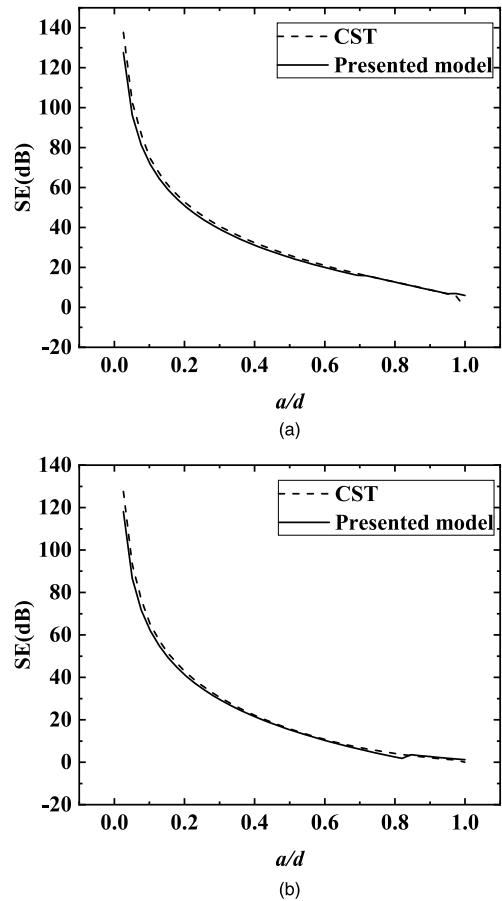


FIGURE 14. Comparison of the SE from full-wave simulation and expressions of different frequencies: (a) $f = 1\text{GHz}$, (b) $f = 3\text{GHz}$.

IV. CONCLUSION

The shielding effectiveness prediction of the periodic aperture array on an infinite conducting plane against a plane electromagnetic wave is studied in this paper. A multi-stage model carried out by bridging the small aperture model and the wire mesh model is presented to calculate the shielding effectiveness.

1) The multi-stage model is based on the piecewise function covering aperture ratio from 0 to 1. When the frequency is higher than the critical frequency, two-stage model is applied. The small aperture model is adopted for the aperture rate less than the critical rate k . Otherwise, the wire mesh model is adopted. When the frequency is lower than the critical frequency, the small aperture model is adopted for the aperture rate below 0.7, the wire mesh model otherwise for the aperture rate above 0.95, and tapers linearly with the rate increasing from 0.7 to 0.95.

2) With perpendicular polarization, the SE is proportional to $\cos\theta$. The SE increases as the angle of incidence increases. With parallel polarization, the relationship between SE and θ is relatively complicated. On the whole, the SE increases as the angle of incidence decreases.

3) For the case that the thickness is not particularly large (not larger than 2mm), the waveguide effect is considered for the small aperture model, and the modified opening width a_{eff}

is applied for the wire mesh model. There is little effect on thickness for the wire mesh model.

4) When the frequency exceeds 3.75GHz, the small aperture model is no longer applicable. In this case, the SE of large apertures is low, which is not feasible for practical application. Therefore, $\lambda \geq 2d$ is the upper-limit frequency of the multi-stage model.

5) For other aperture shape, the small aperture model is still applicable only if the corresponding magnetic polarization is given; The wire mesh model is also feasible only if the distance used in the impedance formula is replaced by that between the neighbor wire parallel to the electric field. The calculations for a rectangular opening with an aspect ratio of 2 indicates that although the multi-stage model turns poor applicability, the consistency with full-wave simulation is still good.

REFERENCES

- [1] L. G. García-Pérez et al., "Time-domain shielding effectiveness of enclosures against a plane wave excitation," *IEEE Trans. Electromagn. Compat.*, vol. 59, no. 3, pp. 789–796, Jun. 2017.
- [2] R. Valente, C. De Ruijter, D. Vlasveld, S. Van Der Zwaag, and P. Groen, "Setup for EMI shielding effectiveness tests of electrically conductive polymer composites at frequencies up to 3.0 GHz," *IEEE ACCESS*, vol. 5, pp. 16665–16675, 2017.
- [3] A. Frikha, M. Bensetti, F. Duval, N. Benjelloun, F. Lafon, and L. Pichon, "A new methodology to predict the magnetic shielding effectiveness of enclosures at low frequency in the near field," *IEEE Trans. Magn.*, vol. 51, no. 3, Mar. 2015, Art. no. 8000404.
- [4] E. Mohammadi, P. Dehkhoda, A. Tavakoli, and B. Honarbakhsh, "Shielding effectiveness of a metallic perforated enclosure by mesh-free method," *IEEE Trans. Electromagn. Compat.*, vol. 58, no. 3, pp. 758–765, Jun. 2016.
- [5] R. Kiebertz and A. Ishimaru, "Aperture fields of an array of rectangular apertures," *IRE Trans. Antennas Propag.*, vol. 10, no. 6, pp. 663–671, Nov. 1962.
- [6] B. J. Rubin and H. L. Bertoni, "Reflection from a periodically perforated plane using a subsectional current approximation," *IEEE Trans. Antennas Propag.*, vol. AP-31, no. 6, pp. 829–836, Nov. 1983.
- [7] W. Wallyn, D. D. Zutter, and H. Rogier, "Prediction of the shielding and resonant behavior of multisection enclosures based on magnetic current modeling," *IEEE Trans. Electromagn. Compat.*, vol. 44, no. 1, pp. 130–138, Feb. 2002.
- [8] P. Dehkhoda, A. Tavakoli, and R. Moini, "An efficient and reliable shielding effectiveness evaluation of a rectangular enclosure with numerous apertures," *IEEE Trans. Electromagn. Compat.*, vol. 50, no. 1, pp. 208–212, Feb. 2008.
- [9] M. P. Robinson et al., "Analytical formulation for the shielding effectiveness of enclosures with apertures," *IEEE Trans. Electromagn. Compat.*, vol. 40, no. 3, pp. 240–248, Aug. 1998.
- [10] T. Y. Otoshi, "A study of microwave leakage through perforated flat plates," *IEEE Trans. Microw. Theory Tech.*, vol. MTT-20, no. 3, pp. 235–236, Mar. 1972.
- [11] S. Tretyakov, "Periodical structures, arrays and meshes," in *Analytical Modeling in Applied Electromagnetics*. Boston, USA: Artech House, 2003, pp. 86–88.
- [12] K. F. Casey, "Electromagnetic shielding behavior of wire-mesh screens," *IEEE Trans. Electromagn. Compat.*, vol. EMC-30, no. 3, pp. 298–306, Aug. 1988.
- [13] MWS. Framingham, MA, USA, (2015). *CST-Computer Simulation Technology*, 2011. [Online]. Available: <http://www.cst.com/Content/Products/MWS/Overview.aspx>
- [14] S. B. Cohn, "Determination of aperture parameters by electrolytic-tank measurements," *Proc. IRE*, vol. 39, no. 11, pp. 1416–1421, Nov. 1951.
- [15] L. H. Hemming, "Applying the waveguide below cut-off principle to shielded enclosure design," in *Presented IEEE Int. Symp. Electromagn. Compat.*, Aug. 1992, pp. 287–289. [Online]. Available: <https://ieeexplore.ieee.org/document/626096?arnumber=626096>
- [16] S.-Y. Hyun, I. Jung, I.-P. Hong, C. Jung, E.-J. Kim, and J.-G. Yook, "Modified sheet inductance of wire mesh using effective wire spacing," *IEEE Trans. Electromagn. Compat.*, vol. 58, no. 3, pp. 911–914, Jun. 2016.



WANXIN BAI was born in Fujian, China, in 1994. She received the B.Sc. degree in hydrology and water resources engineering from North China Electric Power University (NCEPU), Beijing, China, in 2017, where she is currently pursuing the M.A. Eng. degree in electrical engineering. Her research interests include electromagnetic shielding techniques and the electromagnet compatibility in power systems.



ANQI GUO was born in Jiangxi, China, in 1994. She received the B.Sc. degree in electrical engineering and its automation from North China Electric Power University, Baoding, China, in 2016, where she is currently pursuing the M.A. Eng. degree in electrical theory and new technology. Her research interests include electromagnetic shielding techniques and the grounding techniques in power systems.



TIANLE LI was born in Hebei, China, in 1993. He received the B.Sc. degree in electrical engineering from North China Electric Power University, Beijing, China, in 2015, where he is currently pursuing the M.A. Eng. degree. His research interests include electromagnetic shielding techniques and the electromagnet compatibility in power systems.



RUIQI CHENG was born in Hebei, China, in 1995. She received the B.Sc. degree in hydrology and water resources engineering from North China Electric Power University (NCEPU), Beijing, China, in 2017, where she is currently pursuing the M.A. Eng. degree in electrical engineering. Her research interest includes the electromagnetic compatibility in power systems.



CHONGQING JIAO was born in Hubei, China, in 1981. He received the B.Sc. degree in geophysics from the Chinese University of Geosciences, Wuhan, China, and the Ph.D. degree in physical electronics from the Institute of Electronics, Chinese Academy of Sciences, Beijing, China, in 2002 and 2007, respectively. He is currently an Associate Professor of electrical and electronic engineering with North China Electric Power University, Beijing. His research interests include electromagnetic theory and applications, and the EMC in power systems.

• • •